*Biochimica et Biophysica Acta* 806 (1985) 374–388
Elsevier

BBA 41713

# The effects of cation-induced and pH-induced membrane stacking on chlorophyll fluorescence decay kinetics

Kerry K. Karukstis * and Kenneth Sauer **

*Department of Chemistry and Laboratory of Chemical Biodynamics, Lawrence Berkeley Laboratory, University of California, Berkeley, CA 94720 (U.S.A.)*

(Received July 31st, 1984)
(Revised manuscript received October 19th, 1984)

Key words: Cation effect; Chlorophyll fluorescence; Thylakoid stacking; pH effect; (Spinach chloroplast)

**We have compared the effects of thylakoid membrane appression by electrostatic screening and by charge neutralization on the room-temperature chlorophyll fluorescence decay kinetics of broken spinach chloroplasts. Monovalent and divalent metal cations induce both a structural differentiation of thylakoid membranes and a lateral segregation of pigment-protein complexes. These phenomena have distinct effects on the $F_0$- and $F_{max}$-level chlorophyll fluorescence decay kinetics at different levels of added cation. We further find specific cation effects, particularly on a 1–2 ns decay component at the $F_{max}$ fluorescence level, that are proposed to be related to the effectiveness of electrostatic screening as determined by the hydrated metal ionic radius. Distinct pH-induced effects on chlorophyll fluorescence decay kinetics are associated with the alternative mechanism of electrostatic neutralization to induce membrane stacking. These observations are used to construct a model of chlorophyll fluorescence emission that accounts for the variable kinetics and multiexponential character of the fluorescence decay upon membrane appression.**

## Introduction

The surface-electrical properties of thylakoid membranes control a number of photosynthetic phenomena including chlorophyll fluorescence, thylakoid stacking, membrane-conformational changes and electron transport [1,2]. The net negative electrical charge of the thylakoid membrane surface at physiological pH is associated with membrane proteins [2,3], specifically the carboxyl groups of glutamic- and aspartic-acid residues [4,5]. Variations in the membrane-surface charge density, experimentally controlled by the ionic composition of the chloroplast suspension medium, have been intrinsically probed with measurements of chlorophyll fluorescence [1,6–11] and correlated with modifications in the extent of thylakoid membrane stacking and in the distribution of chlorophyll-protein complexes [12]. These closely related phenomena reflect changes in the balance of electrostatic and electrodynamic forces which exist between protein complexes and between adjacent membrane surfaces [12,13].

Cation-induced membrane appression preserves the in vivo structural differentiation of thylakoid

* Present address: Department of Chemistry, Harvey Mudd College, Claremont, CA, U.S.A.
** To whom correspondence should be addressed.

Abbreviations: Chl, chlorophyll; $F_0$, background fluorescence, level of chlorophyll fluorescence with Photosystem II electron acceptor Q oxidized; $F_{max}$, maximum fluorescence, level of chlorophyll fluorescence with Photosystem II electron acceptor Q reduced; $F_{var}$, variable fluorescence, defined as the quantity $F_{max} - F_0$; Hepes, 4-(2-hydroxyethyl)-1-piperazineethanesulfonic acid; LHCP, light-harvesting chlorophyll *a*/*b*-protein complex; Mes, 4-morpholineethanesulfonic acid; PS, Photosystem; LHCP, light-harvesting chlorophyll *a*/*b*-protein.

membranes into stacked (grana lamellae) and exposed (stroma lamellae) regions [14–17] with a lateral distribution of the supramolecular chlorophyll-protein complexes between grana and stroma regions [18–21]. In the grana partitions, Photosystem II (PS II) and light-harvesting chlorophyll *a*/*b*-protein (LHCP) complexes are highly enriched; in contrast, stroma-exposed thylakoids are enriched in Photosystem I (PS I) complexes. At least a portion of the observed increase in chlorophyll fluorescence intensity upon membrane appression presumably reflects alterations in the degree of energy transfer from PS II to PS I complexes, arising from a spatial separation of photosystems upon exclusion of PS I from grana stacks [12,22]. Incubation of chloroplasts in media of low-ionic strength fully unstacks the thylakoid membranes [14,22] and randomly distributes PS I, PS II and LHCP complexes along the membrane plane [19,20]. The absence of discrete domains of pigment-protein complexes reestablishes energy transfer between photosystems and lowers the observed chlorophyll fluorescence intensity [12,22].

Theoretical analyses suggest that electrostatic screening of fixed negative charges on the thylakoid membrane surface by added cations is a mechanism for the reversible stacking of chloroplast membranes, for aggregation of complexes within the membrane plane and for the associated fluorescence variations [12,22]. A differential effect in restacking of monovalent and divalent cations, with divalent cations (2–5 mM) more effective that monovalent ions (50–100 mM) in this reconstitution [6–8,12], is observed; however, a general lack of specificity among species of a particular charge group is generally considered to be the rule [12,23].

Grana formation is also induced by lowering the pH of the chloroplast-suspending medium to 5.1–5.4 [13,24], which is still above the isoelectric point of chloroplast membranes [3,4,13,24]. Proton-induced stacking is envisaged to occur by a mechanism involving the electrostatic neutralization of surface charges by the protonation of surface-exposed carboxyl groups [24,25]. Surface charge neutralization is apparently sufficient to permit the membranes to approach each other and stack, retaining a random distribution of PS I, PS II and LHCP complexes in the membrane. Furthermore, charge neutralization does not induce so substantial a variation in chlorophyll fluorescence intensity as does cation screening, presumably because energy transfer from PS II to PS I is maintained in the absence of domain formation [12,23].

A recent study [24] suggests that $La^{3+}$ cations can be involved in both electrostatic screening and charge neutralization mechanisms. At low concentrations (up to 20 $\mu$M), $La^{3+}$ ions mimic the action of screening cations in promoting grana formation and in increasing chlorophyll fluorescence. At higher concentrations, $La^{3+}$ ions are believed to bring about surface charge neutralization and the accompanying membrane stacking, with a less pronounced increase in chlorophyll fluorescence [24,25].

The objective of the present investigation is to compare the effects of membrane appression by electrostatic screening and by charge neutralization on the room-temperature chlorophyll fluorescence decay kinetics of broken spinach chloroplasts. Our investigation focuses on the following four questions. (1) Can we distinguish differences between monovalent and divalent cation effects on the fluorescence decay kinetics? (2) Can we discern variations in the cation effects of metals within the same valency group? (3) Can we characterize distinct cation-induced or pH-induced membrane stacking effects on chlorophyll fluorescence decay kinetics? (4) Can we differentiate between screening and neutralization effects of $H^+$ and $La^{3+}$ on chlorophyll fluorescence decay kinetics?

To attempt to answer these questions, we present selected concentration dependence studies of cation (monovalent, divalent, $H^+$, and $La^{3+}$ ions) effects on spinach chloroplasts, analogous to the $Mg^{2+}$ investigation reported by Nairn et al. [26] in which the addition of $Mg^{2+}$ has distinct effects on the chlorophyll fluorescence decay kinetics at different levels of added cation. Our results demonstrate that the mechanism of membrane stacking clearly influences the measured chlorophyll fluorescence decay kinetics. Furthermore, the extent of variation of some fluorescence decay parameters under conditions of electrostatic screening is dependent on ion valency and size. We use these observations of variable kinetics to construct a model for the origin of the chlorophyll fluorescence decay components.

## Materials and Methods

For metal-cation studies, chloroplasts were isolated from freshly harvested growth-chamber spinach in a medium containing 0.4 M sucrose/50 mM Hepes-NaOH (pH 7.5)/10 mM NaCl. After centrifugation at 6000 × *g* for 10 min and washing with the same medium, the chloroplasts were resuspended in a medium of 0.1 M sucrose/10 mM Hepes-NaOH (pH 7.5)/10 mM NaCl. Following centrifugation at 6000 × *g* for 10 min, the pellet was resuspended in the same medium, kept in the dark for 20 min at 0°C, and then a similar centrifugation step was performed. Portions of this final pellet were then resuspended in a medium of 0.1 M sucrose and 10 mM Hepes-NaOH (pH 7.5) at the desired concentration of metal cation to give approx. 1 mg Chl per ml. The chloroplasts were allowed to equilibrate in these buffers for 1 h to ensure complete changes in stacking and reorganization of chlorophyll-protein complexes [25]. For fluorescence measurements the chloroplast suspension was diluted with the final buffer to a concentration of 10 μg Chl per ml.

For pH measurements, the chloroplasts were prepared as above except that the final pellet was resuspended in a medium poised at the desired pH. The procedure of pH poising, adopted from a previously described method [24], involved the suspension of the pellet in a final buffer of 0.1 M sucrose, 5 mM $Na^+$ and a combination of 0.1 M Hepes and 0.1 M Mes, adjusted with HCl to the proper pH value.

The fluorescence excitation source was a Spectra Physics synchronously pumped mode-locked dye laser (SP 171 argon ion laser, SP 362 mode locker and modified SP 375 dye laser). Chloroplast samples were excited with pulses of 8 ps half-maximum full-width duration at 620 nm and at 80 MHz repetition frequency. The maximum laser pulse intensity ($1 \cdot 10^7$ photons per $cm^2$) was attenuated with neutral density filters for intensity-dependence experiments. Fluorescence was detected at right angles at 680 nm using an RCA 31034A photomultiplier tube. The single-photon timing system and numerical analysis methods have been described previously [27–30]. All fluorescence decay data were resolved into a sum of exponential decays with a lifetime resolution limit of 50 ps. In general, as previously observed [26,27], the kinetics of the chlorophyll fluorescence emission is best described by three exponential components (termed the 'slow', 'middle' and 'fast' decay components), both in the presence and absence of added cations. The degree of variability in the deconvoluted lifetimes for replicate samples measured during the course of a single experiment is generally ±10 ps for a fluorescence decay component in the 50–200 ps range, ±25 ps in the 500 ps–1 ns range, ±50 ps in the 1–2 ns range, and ±150 ps in the 2–4 ns range. Plots of the deviations of the measured fluorescence decay from the results of the deconvolution indicate how well the presumed decay law matches the experimental data. We may further evaluate the goodness of fit by the reduced chi-square ($\chi^2_R$) test, with values near 1.00 (typically in the range 1.00–1.25) indicating that the residuals of the measured curve about the fitted curve are normally distributed and due only to statistical noise [31].

For fluorescence measurements corresponding to open reaction centers ($F_0$), chloroplasts were dark-adapted for 10 min and then low intensities of excitation ($1 \cdot 10^5$ photons per $cm^2$ per pulse) were used to maintain the $F_0$ level and to prevent steady-state reduction of Q [32]. To produce closed reaction centers, the laser intensity was increased 100-fold. All laser pulse energies used were sufficiently low to exclude any contribution from biexcitonic annihilation processes [33,34].

## Results

### *Monovalent cation effects on $F_0$- and $F_{max}$-level fluorescence*

Table I presents a comparison of the effect of the monovalent cations $Li^+$, $Na^+$ and $K^+$ at 100 mM concentration on $F_0$ and $F_{max}$ total and decay component fluorescence yields of spinach chloroplasts. At the $F_0$ fluorescence level, no difference in total yield is observed among the various cations. However, with increasing metal-ionic radius ($Li^+ < Na^+ < K^+$) $\phi_{slow}$ increases by more than 2-fold and $\phi_{middle}$ decreases by 20%. Changes in $\phi_{fast}$ are within the experimental error of our measurements. The $F_{max}$ total fluorescence yield decreases with the sequence $Li^+ > Na^+ > K^+$, with $\phi_{total}$ for $K^+$ only 50% of that for $Li^+$. The dif-

TABLE I

RELATIVE FLUORESCENCE YIELDS OF SPINACH CHLOROPLASTS INCUBATED IN MONOVALENT CATION-ENRICHED MEDIA

These data show the effects of adding 100 mM monovalent cation at both the $F_0$ and $F_{max}$ levels. All results are for chloroplasts isolated from a single set of spinach leaves. The yield figures are normalized such that $\phi_{total}$ at $F_{max}$ in the presence of 5 mM $Mg^{2+}$ equals 100 (see Table III).

| Cation | $\phi_{slow}$ | $\phi_{middle}$ | $\phi_{fast}$ | $\phi_{total}$ |
|---|---|---|---|---|
| $F_0$-fluorescence level | | | | |
| $Li^+$ | 3 | 14 | 3 | 20 |
| $Na^+$ | 4 | 13 | 3 | 20 |
| $K^+$ | 7 | 12 | 2 | 21 |
| $F_{max}$-fluorescence level | | | | |
| $Li^+$ | 65 | 12 | 3 | 80 |
| $Na^+$ | 55 | 12 | 3 | 70 |
| $K^+$ | 26 | 12 | 2 | 40 |

ferences in $\phi_{total}$ for the various cations are accounted for by variations in $\phi_{slow}$.

The corresponding lifetimes of the fluorescence decay components at $F_0$ and $F_{max}$ are summarized in Table II. At $F_0$, variations in the fluorescence lifetimes with cation species are considered to be negligible and within the lifetime resolution of our instrument. At $F_{max}$, both $\tau_{slow}$ and $\tau_{middle}$ decrease significantly with increasing metal-ionic radius.

TABLE II

FLUORESCENCE LIFETIMES OF SPINACH CHLOROPLASTS INCUBATED IN MONOVALENT CATION-ENRICHED MEDIA

These data show the effects of adding 100 mM monovalent cation at both the $F_0$ and $F_{max}$ levels. All results are for the chloroplasts of Table I.

| Cation | $\tau_{slow}$ (ps) | $\tau_{middle}$ (ps) | $\tau_{fast}$ (ps) |
|---|---|---|---|
| $F_0$-fluorescence level | | | |
| $Li^+$ | 1100 | 450 | 105 |
| $Na^+$ | 1000 | 425 | 100 |
| $K^+$ | 950 | 450 | 90 |
| $F_{max}$-fluorescence level | | | |
| $Li^+$ | 1950 | 700 | 120 |
| $Na^+$ | 1700 | 625 | 90 |
| $K^+$ | 1400 | 525 | 95 |

TABLE III

RELATIVE FLUORESCENCE YIELDS OF SPINACH CHLOROPLASTS INCUBATED IN DIVALENT CATION-ENRICHED MEDIA

These data show the effects of adding 5 mM divalent cation at both the $F_0$ and $F_{max}$ levels. All results are for chloroplasts isolated from a single set of spinach leaves. The yield figures are normalized such that $\phi_{total}$ at $F_{max}$ in the presence of 5 mM $Mg^{2+}$ equals 100.

| Cation | $\phi_{slow}$ | $\phi_{middle}$ | $\phi_{fast}$ | $\phi_{total}$ |
|---|---|---|---|---|
| $F_0$-fluorescence level | | | | |
| $Mg^{2+}$ | 2 | 15 | 3 | 20 |
| $Ca^{2+}$ | 2 | 14 | 3 | 19 |
| $Ba^{2+}$ | 2 | 12 | 3 | 17 |
| $F_{max}$-fluorescence level | | | | |
| $Mg^{2+}$ | 88 | 10 | 2 | 100 |
| $Ca^{2+}$ | 67 | 15 | 2 | 84 |
| $Ba^{2+}$ | 39 | 14 | 2 | 55 |

*Divalent cation effects on $F_0$- and $F_{max}$-level fluorescence*

Table III lists the $F_0$ and $F_{max}$ total and decay component fluorescence yields for spinach chloroplasts isolated in suspending media enriched in each of the divalent cations $Mg^{2+}$, $Ca^{2+}$ and $Ba^{2+}$ at a concentration of 5 mM. The differences in $\phi_{total}$ ($Mg^{2+} > Ca^{2+} > Ba^{2+}$) arise from variations in $\phi_{middle}$. At $F_{max}$, as in the monovalent series,

TABLE IV

FLUORESCENCE LIFETIMES OF SPINACH CHLOROPLASTS INCUBATED IN DIVALENT CATION-ENRICHED MEDIA

These data show the effects of adding 5 mM divalent cation at both the $F_0$ and $F_{max}$ levels. All results are for the chloroplasts of Table III.

| Cation | $\tau_{slow}$ (ps) | $\tau_{middle}$ (ps) | $\tau_{fast}$ (ps) |
|---|---|---|---|
| $F_0$-fluorescence level | | | |
| $Mg^{2+}$ | 1000 | 415 | 95 |
| $Ca^{2+}$ | 1100 | 360 | 75 |
| $Ba^{2+}$ | 1450 | 400 | 105 |
| $F_{max}$-fluorescence level | | | |
| $Mg^{2+}$ | 2000 | 675 | 90 |
| $Ca^{2+}$ | 1850 | 725 | 105 |
| $Ba^{2+}$ | 1600 | 650 | 120 |

$\phi_{total}$ decreases with increasing divalent metal ionic radius, with $\phi_{total}$ in the presence of $Mg^{2+}$ almost twice that present in $Ba^{2+}$-enriched media. Variations in $\phi_{slow}$ make the most significant contribution to the differences in $\phi_{total}$.

The corresponding fluorescence lifetimes measured at $F_0$ and $F_{max}$ are detailed in Table IV. No significant variation in $\tau_{middle}$ or $\tau_{fast}$ is observed at either $F_0$ or $F_{max}$ with varying cation identity. A 40% increase in $\tau_{slow}$ occurs at $F_0$ for the sequence $Mg^{2+} < Ca^{2+} < Ba^{2+}$. At $F_{max}$ decreases occur in $\tau_{slow}$ in the order $Mg^{2+} > Ca^{2+} > Ba^{2+}$.

*Fluorescence decay kinetics as a function of monovalent and divalent ion concentration*

The dependence of the $F_0$ total and decay component fluorescence yields and lifetimes on $Na^+$ and $K^+$ concentrations are presented in Figs. 1 and 2, respectively. The corresponding effects of

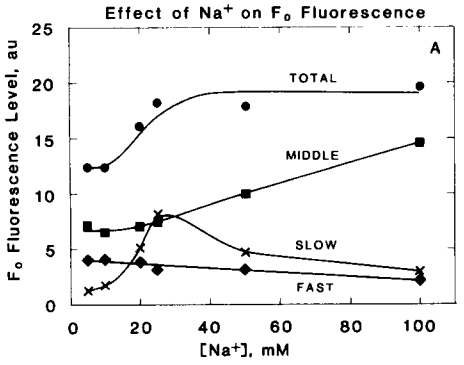


Fig. 1. Total yield and yields of the components of the fluorescence decay of spinach chloroplasts at $F_0$ (A) as a function of $Na^+$ concentration and (B) as a function of $K^+$ concentration. The symbols are defined as follows: total yield (●); yield of the slow component (×); yield of the middle component (■); and yield of the fast component (◆).

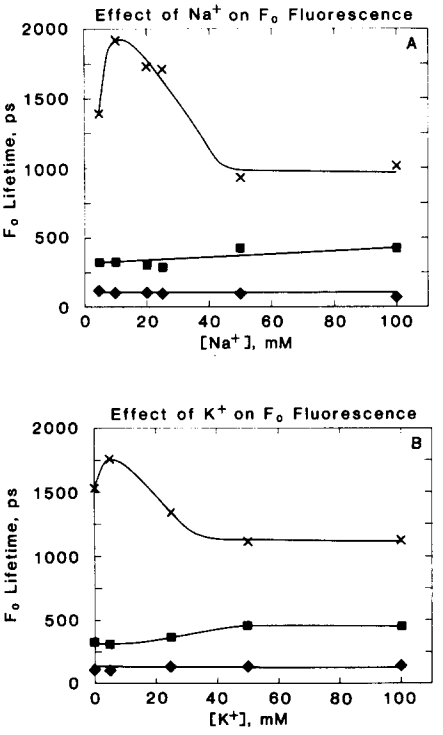


Fig. 2. Lifetimes of the components of the fluorescence decay of spinach chloroplasts at $F_0$ (A) as a function of $Na^+$ concentration and (B) as a function of $K^+$ concentration. The symbols are defined as follows: lifetime of the slow component (×); lifetime of the middle component (■); and lifetime of the fast component (◆).

$Ca^{2+}$ concentration are summarized in Fig. 3. An increase occurs in $\phi_{total}$ with increasing ion concentration, saturating at about 25 mM for both $Na^+$ and $K^+$ and reaching a maximum at 0.25 mM $Ca^{2+}$ (but decreasing with additional $Ca^{2+}$). Complex changes in the individual decay components are observed. In particular, $\phi_{slow}$ increases dramatically (6–10-fold increase) at 25 mM $Na^+$ and $K^+$ and 0.25 mM $Ca^{2+}$, followed by a decrease to the initial value or lower with additional cation. A doubling of $\phi_{middle}$ occurs at concentrations above 25 mM monovalent ion and 0.75 mM divalent ion, with small decreases in $\phi_{fast}$ observed over the range of concentrations studied. The most dramatic changes in fluorescence lifetime are observed for $\tau_{slow}$, with an increase from 1400 ps at low ion concentrations to a maximum of 1900 ps for 10 mM $Na^+$, 1750 ps for 5 mM $K^+$ (total

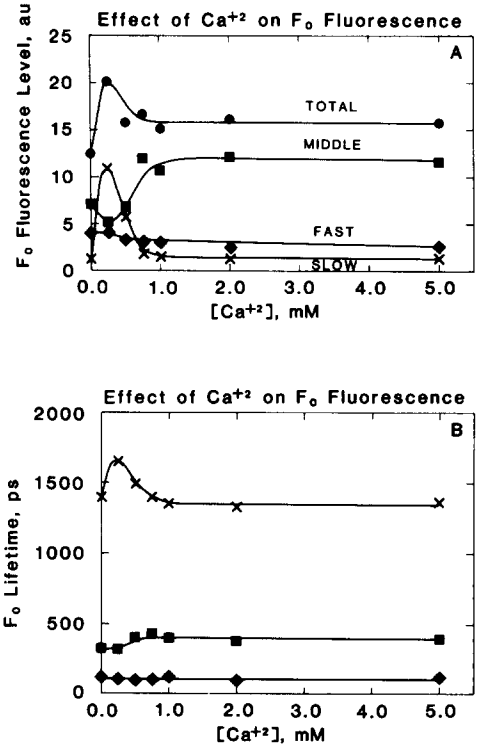


Fig. 3. (A) Total yield and yields of the fluorescence decay components of spinach chloroplasts at $F_0$ as a function of $Ca^{2+}$ concentration. (B) Lifetimes of the fluorescence decay components of spinach chloroplasts at $F_0$ as a function of $Ca^{2+}$ concentration. The symbols are defined as in Figs. 1 and 2.

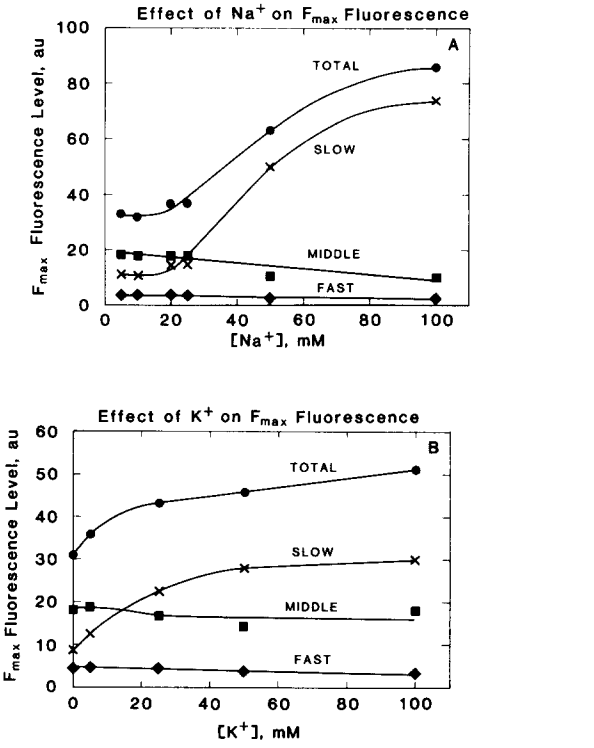


Fig. 4. Total yield and yields of the components of the fluorescence decay of spinach chloroplasts at $F_{max}$ (A) as a function of $Na^+$ concentration and (B) as a function of $K^+$ concentration. The symbols are defined as in Fig. 1.

monovalent ion concentration, 10 mM), and 1700 ps at 0.25 mM $Ca^{2+}$.

The effects of the concentration level of $Na^+$ and $K^+$ on the $F_{max}$ total fluorescence and decay component yields and lifetimes are plotted in Figs. 4 and 5. Fig. 6 presents analogous data for $Ca^{2+}$ studies. An increase in $\phi_{total}$ predominantly arises from a change in $\phi_{slow}$, with $Na^+$ and $Ca^{2+}$ exhibiting a 7-fold increase in $\phi_{slow}$ and $K^+$ a 3-fold increase. A small (up to 50%) decrease in $\phi_{middle}$ is observed for all ions, but variations in $\phi_{fast}$ are within the experimental error of our measurements. Pronounced increases in $\tau_{slow}$ and $\tau_{middle}$ are noted, but little effect of ion concentration on $\tau_{fast}$ is detected.

*Fluorescence decay kinetics as a function of pH*

Figs. 7 and 8 show the effect of the pH of the chloroplast suspending medium on the $F_0$ and $F_{max}$ level fluorescence decay kinetics, respectively. As the pH is lowered from 7.6 to 5.7, $\phi_{total}$ increases 50% and then subsequently decreases to almost its original value as the pH is lowered to 4.3. The yield of the slow phase follows the same trends. A 40% increase in $\phi_{middle}$ is measured during the pH transition from pH 5.7 to 5.1. A slight decrease in $\phi_{fast}$ is also apparent as the pH is lowered. Variations in the pH of the chloroplast-suspending medium have little effect on the $F_0$-level lifetimes of the middle and fast fluorescence decay components, as plotted in Fig. 7B. However, $\tau_{slow}$ shows complex pH-dependent behavior.

At $F_{max}$, a doubling in $\phi_{total}$ occurs as the pH is lowered from 7.6 to 5.1, with a decrease to the mimimum level at pH 4.3. A similar pH dependence is observed for $\phi_{slow}$. A decline in both $\phi_{middle}$ and $\phi_{fast}$ ensues during the pH lowering to 4.3. Only $\tau_{slow}$ is affected by pH variation at $F_{max}$,

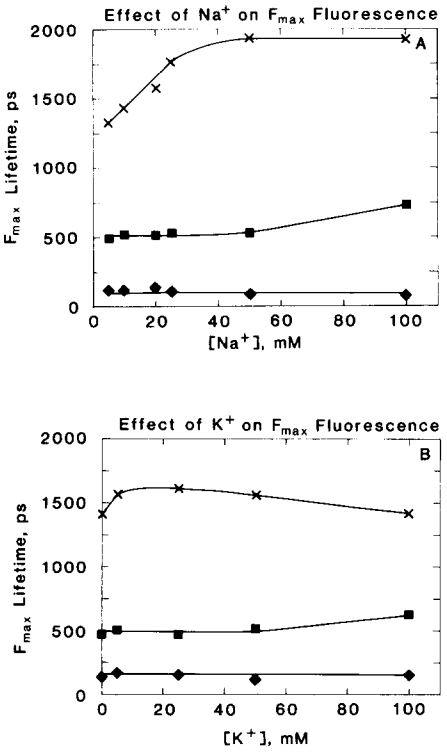


Fig. 5. Lifetimes of the components of the fluorescence decay of spinach chloroplasts at $F_{max}$ (A) as a function of $Na^+$ concentration and (B) as a function of $K^+$ concentration. The symbols are defined as in Fig. 2.

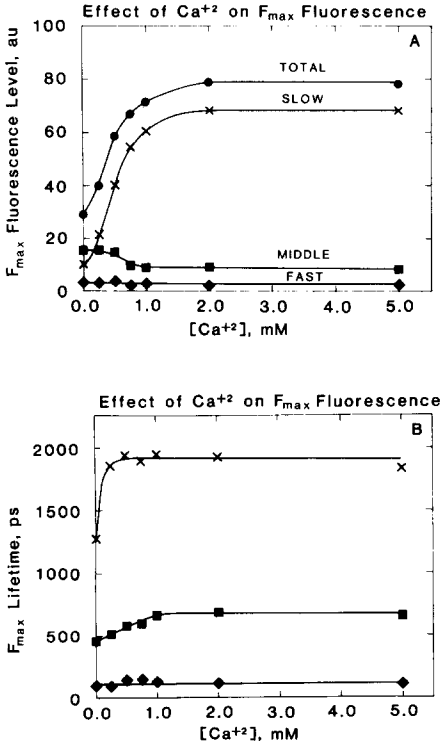


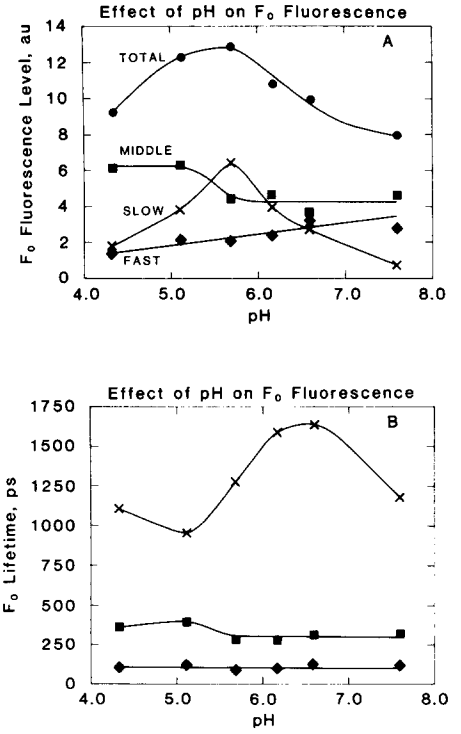


Fig. 7. (A) Total yield and yields of the fluorescence decay components of spinach chloroplasts at $F_0$ as a function of pH of the suspending medium. (B) Lifetimes of the fluorescence decay components of spinach chloroplasts at $F_0$ as a function of pH of the suspending medium. The symbols are defined as in Figs. 1 and 2.

increasing from 1100 (pH 7.6) to 1550 ps (pH 5.1), and then markedly falling to 900 ps (pH 4.3). The value of $\tau_{middle}$ remains constant at approx. 400 ps and that of $\tau_{fast}$ averages about 100 ps for the pH interval 7.6–4.3.

*Fluorescence decay kinetics as a function of $La^{3+}$ concentration*

The effects of $La^{3+}$ over the concentration range 0–100 $\mu$M on the $F_0$ and $F_{max}$ fluorescence decay kinetics are shown in Figs. 9 and 10, respectively. Increases in $\phi_{total}$ and $\phi_{slow}$ occur with the addition of 5 $\mu$M $La^{3+}$, followed by decreases in both these yields to approximately their initial values with the

Fig. 6. (A) Total yield and yields of the fluorescence decay components of spinach chloroplasts at $F_{max}$ as a function of $Ca^{2+}$ concentration. (B) Lifetimes of the fluorescence decay components of spinach chloroplasts at $F_{max}$ as a function of $Ca^{2+}$ concentration. The symbols are defined as in Figs. 1 and 2.

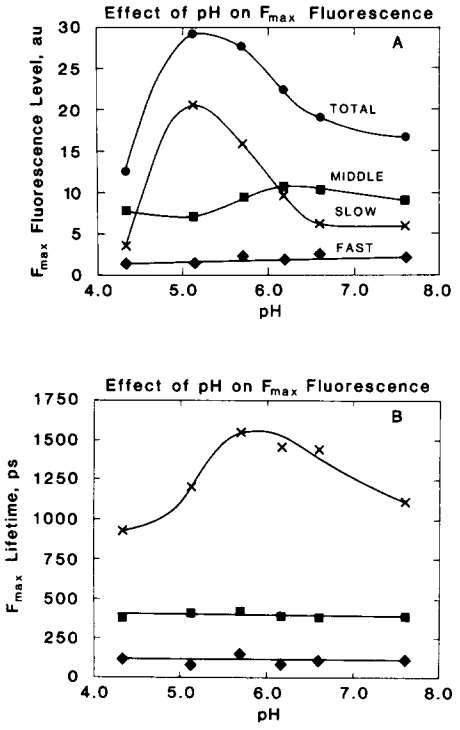


Fig. 8. (A) Total yield and yields of the fluorescence decay components of spinach chloroplasts at $F_{max}$ as a function of pH of the suspending medium. (B) Lifetimes of the fluorescence decay components of spinach chloroplasts at $F_{max}$ as a function of pH of the suspending medium. The symbols are defined as in Figs. 1 and 2.

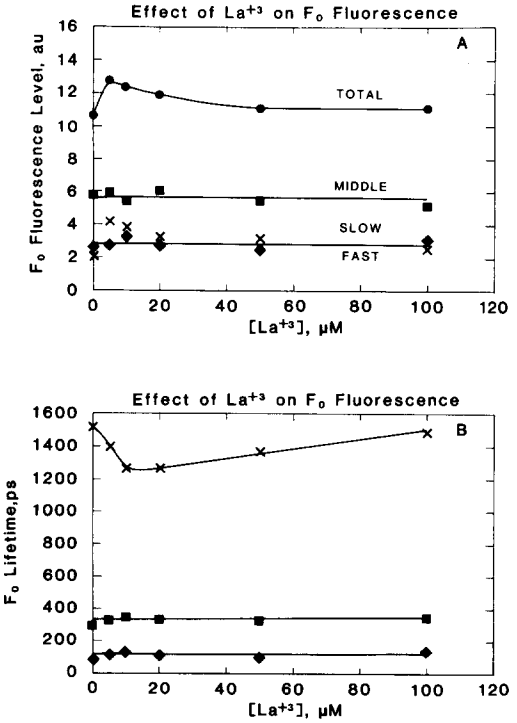


Fig. 9. (A) Total yield and yields of the fluorescence decay components of spinach chloroplasts at $F_0$ as a function of $La^{3+}$ concentration. (B) Lifetimes of the fluorescence decay components of spinach chloroplasts at $F_0$ as a function of $La^{3+}$ concentration. The symbols are defined as in Figs. 1 and 2.

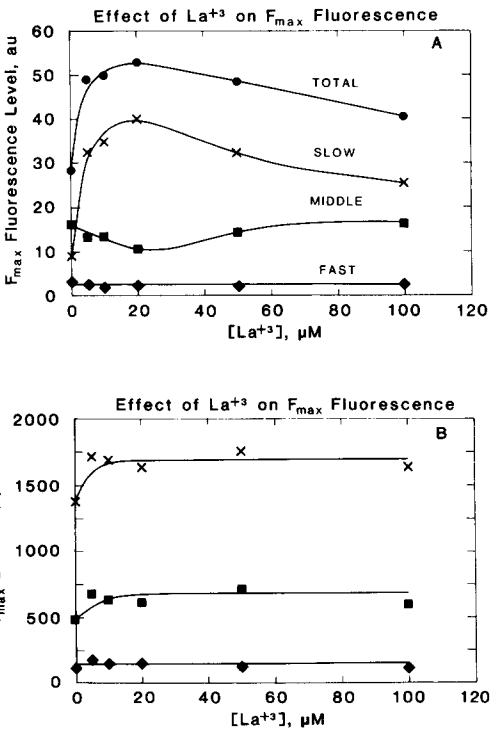


Fig. 10. (A) Total yield and yields of the fluorescence decay components of spinach chloroplasts at $F_{max}$ as a function of $La^{3+}$ concentration. (B) Lifetimes of the fluorescence decay components of spinach chloroplasts at $F_{max}$ as a function of $La^{3+}$ concentration. The symbols are defined as in Figs. 1 and 2.

addition of 100 $\mu$M $La^{3+}$. Variations in the $F_0$-level values of $\phi_{middle}$ and $\phi_{fast}$ with changes in $La^{3+}$ concentration are considered negligible. Fig. 9B shows that $\tau_{middle}$ and $\tau_{fast}$ are independent of $La^{3+}$ concentration at the $F_0$ fluorescence level. A decrease occurs in $\tau_{slow}$ from 1500 ps in the absence of $La^{3+}$ to 1250 ps in the range of 10–20 $\mu$M $La^{3+}$, followed by a return to 1500 ps with 100 $\mu$M $La^{3+}$.

At $F_{max}$, the addition of $La^{3+}$ increases $\phi_{total}$, with a maximum effect occurring at 20 $\mu$M $La^{3+}$; higher levels of $La^{3+}$ (50–100 $\mu$M) decrease $\phi_{total}$ about 25%. Comparable $La^{3+}$ effects were reported for steady-state fluorescence levels [25]. A similar dependence is observed for $\phi_{slow}$. With the

addition of $La^{3+}$ to the chloroplast-suspending medium at $F_{max}$, $\tau_{slow}$ increases from 1400 to 1700 ps, $\tau_{middle}$ increases from 500 to about 650 ps, and $\tau_{fast}$ remains constant with an average value of 130 ps.

## Discussion

*Analysis of cation-specific effects*

An analysis of the data in Tables I–IV reveals variations within a valence group in cation-induced chlorophyll fluorescence decay changes, especially at $F_{max}$. Specifically, we note that the smaller the metal ionic radius, the greater the $F_{max}$ yield and the larger the contribution of $\phi_{slow}$ to the overall fluorescence intensity. Furthermore, although the valence of the metal cation has little influence on the $F_0$-level fluorescence decay kinetics, a significant difference is observed between divalent and monovalent ion effects on the $F_{max}$ total and component fluorescence yields. In particular, the greater the valency for ions of comparable ionic radii, the larger the fluorescence intensity at $F_{max}$ and the more significant the contribution of $\phi_{slow}$ to the total yield.

These points are most easily explained by well-established principles of electrical phenomena at the surface of biological membranes. In particular, for a diffuse electrical layer adjacent to a planar membrane surface having a net negative charge, divalent cations more effectively screen the fixed surface negative charges than do monovalent cations, even for a 10-fold higher concentration of monovalent ions [2]. Furthermore, the effectiveness of an ion to reduce the membrane-surface potential is directly related to its distance of closest approach, determined by the ionic radius and degree of hydration. In this study, the larger the hydrated ionic radius (i.e., the smaller the metal-ionic radius) the more pronounced the effect of the metal ion on the chlorophyll fluorescence yield at $F_{max}$. This observation necessarily implies that more effective electrostatic screening does not always lead to enhanced chlorophyll-fluorescence yields. These results are consistent with the observed fluorescence decrease upon charge neutralization (pH and $La^{3+}$ results) and the accompanying close approach of thylakoid membrane surfaces [24]. A model to support this observation will be proposed below.

We suggest that these differences in cation-induced fluorescence variations were not previously noted in the steady-state fluorescence measurements of Murata et al. [6–8] because these earlier determinations were made after only 5 minutes incubation of the chloroplasts in the cation-enriched suspending medium. As noted by Barber et al. [25], the time-course for complete cation-induced chlorophyll fluorescence changes is substantially longer than a 5 min incubation period, and the full extent of cation effects can be overlooked if there is an inadequate time for complete conformational changes. In the present investigation, the chloroplast suspensions equilibrated for at least 1 h prior to making fluorescence determinations, thus providing adequate time for membrane stacking and pigment-protein lateral diffusion.

Despite cation differences in the extent of fluorescence variation upon membrane stacking, similar behavior in the fluorescence decay kinetics changes can be noted during the course of such grana formation via electrostatic screening. We suggest that such analogous behavior is a consequence of the mechanism for grana formation that is generally independent of the cation used and controlled by electrostatic phenomena. Our ability to sensitively monitor cation-induced variations in chlorophyll fluorescence reveals reasonable differences in cation effects.

*Proposed model of chlorophyll fluorescence emission*

The variable kinetics and multiexponential character of the chlorophyll fluorescence emission measured in these investigations can be used to construct a model for the origin of the fluorescence decay components. The proposed model is presented schematically in Fig. 11. The model is formulated on the assumption of marked lateral heterogeneity in the distribution of the chlorophyll-protein complexes along the thylakoid membrane under conditions of electrostatic screening and the assumption of a random organization of such complexes in a situation of charge neutralization or in unstacked membranes [12,18–20,22]. The designation of $\alpha$- and $\beta$-centers refers to the localization of PS II reaction centers in the partition regions of the grana stacks and in the un-

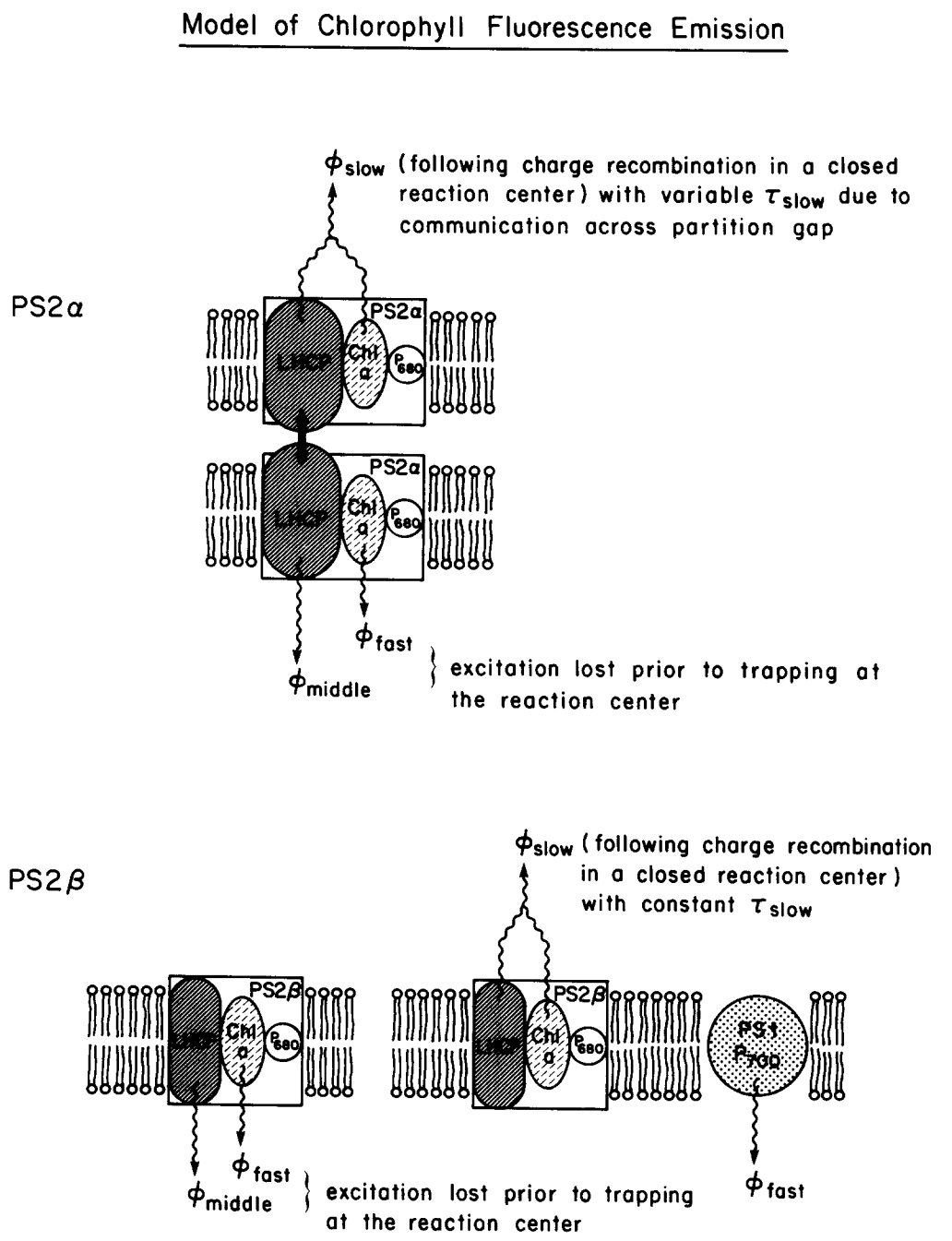


Fig. 11. Proposed model of chlorophyll fluorescence emission at $F_0$ and $F_{max}$ for chlorophyll-protein complexes in grana partitions and stroma-exposed thylakoids. Symbols include: P-680, Photosystem II reaction center; P-700, Photosystem I reaction center; LHCP, light-harvesting chlorophyll *a*/*b*-protein complex; Chl *a*, chlorophyll a core antenna complex; PS2$\alpha$, Photosystem II$\alpha$ units; PS2$\beta$, Photosystem II$\beta$ units.

stacked thylakoids exposed to the aqueous environment of the stroma, respectively [35].

At $F_0$, with PS II reaction centers open to photochemistry, the observed fluorescence emission results predominantly from excitation lost prior to reaching PS II reaction centers. The effectiveness of PS II centers as fluorescence quenchers suggests that a slower decaying component of this $F_0$ emission emanates from the more distant chlorophyll *a/b* light-harvesting complexes rather than from the more tightly coupled chlorophyll *a* core antennae. This assignment assumes, however, that other competitive deexcitation processes (such as nonradiative decay) have similar rate constants for both types of chlorophyll-protein complexes. As a consequence, in the proposed model $\phi_{middle}$ is attributed to a composite of emission from the chlorophyll *a/b* light-harvesting complexes associated with PS II$\alpha$ and II$\beta$ centers. Furthermore, the larger chlorophyll *a/b* antenna size of PS II$\alpha$ units suggests a larger contribution to the $F_0$ emission from the light-harvesting pigment bed of PS II$\alpha$ than from the LHCP of PS II$_\beta$ [34,36]. Assuming that the relative number of $\alpha$ and $\beta$ units remains unchanged during cation addition [35], the increase in $\phi_{middle}$ at $F_0$ with high concentrations of metal cations suggests an increase in the absorption cross-section of PS II$_\alpha$ units, and therefore an increase in the average time for transfer of excitation energy from the light-harvesting chlorophyll *a/b* antenna to the chlorophyll *a* antenna of Photosystem II. This hypothesis is in agreement with a similar proposal for the effect of $Mg^{2+}$ on the $F_0$ level of $\phi_{middle}$ [26].

The fluorescence lifetime of $\phi_{middle}$ is indirectly affected by the photochemical state of reaction centers only when energy transfer is possible. As isolated PS II units or $\beta$-centers of the stromal lamellae are closed, with increasing excitation intensity, no change in $\tau_{middle}$ would be expected in the absence of energy transfer. However, $\phi_{middle}$ would increase with excitation intensity until all PS II reaction centers are closed, because the probability of fluorescence emission prior to reaching the reaction center trap is proportional to the excitation intensity. For communicating PS II units or $\alpha$-centers of granal lamellae, the presence of energy transfer increases the possibility that (1) at low light intensities excitation will be trapped by a reaction center as a consequence of the proximity of many open reaction centers, and (2) at high light intensities excitation will successfully escape an encounter with an open reaction center via energy transfer and therefore avoid trapping. As the path followed by excitation energy to escape trapping lengthens, any potential fluorescence emission will thus exhibit a characteristically longer lifetime (i.e., $\tau_{middle}$ increases as reaction centers are closed). We propose that $\tau_{middle}$ reflects an average fluorescence lifetime for excitation lost prior to reaching the reaction center and which is emitted from the chlorophyll *a/b* light-harvesting complexes of both $\alpha$- and $\beta$-PS II centers. We suggest that the time resolution of our system is such that we cannot distinguish $\tau_{middle}$ ($\alpha$-centers) from $\tau_{middle}$ ($\beta$-centers).

The fast decay component at $F_0$ is attributed to a composite of emission from the chlorophyll *a* antennae closely coupled to PS II units and the light-harvesting pigments of PS I. The cation- and pH-independent lifetime and yield of this decay component are in agreement with the absence of membrane stacking effects on PS II chlorophyll *a* core antenna complexes and the presence of only a small amount of room temperature chlorophyll fluorescence from PS I.

The model of Fig. 11 suggests, as in earlier studies [26,27], that the slow decay component is attributable to fluorescence following charge separation in closed reaction centers ($P^*$-680 $IQ^- \rightarrow P^+$-680 $I^-Q^-$) and a subsequent radical-pair recombination of $P^+$-680 and $I^-$. Excitation arising from the repopulation of the excited singlet state of P-680 ($P^+$-680 $I^-Q^- \rightarrow P^*$-680 $IQ^-$) may be transferred to the antenna chlorophyll molecules and emitted as the slow decay component of fluorescence. On the basis of the present data, we further qualify this assignment to state that in structurally differentiated chloroplasts $\phi_{slow}$ is predominantly emitted via the described mechanism from the LHCP antenna of PS II$\alpha$ units. To support this assignment, we note that the observed increase in $\phi_{slow}$ at $F_{max}$ with the addition to unstacked membranes of metal cations, $H^+$ ions, or $La^{3+}$ ions is in excellent agreement with the 5–7-fold increase in the variable fluorescence yield controlled by $\alpha$-centers as measured by Melis and Ow upon $Mg^{2+}$ addition to unstacked membranes

[35]. As previously hypothesized [25,35], we also suggest here that the observed ion-induced variations in the slow decay component yield arise from a cation-dependent radiationless decay constant ($k_d$) at a closed PS II$\alpha$ reaction center (greater in the absence of metal ions, lower in presence). We propose that the analogous charge recombination decay component from $\beta$-centers constitutes a smaller portion of $\phi_{slow}$ and, furthermore, contributes no cation-dependent variable fluorescence to $\phi_{slow}$, as was also observed by Melis and Ow [35]. We further suggest that distinct values of $\tau_{slow}$ for coexisting $\alpha$- and $\beta$-centers cannot be resolved with the present timing system. Presumably the small amount of $\phi_{slow}$ observed at the $F_0$ fluorescence level indicates that the fluorescence conditions (excitation intensity, collection time and sample preparation) are not quite adequate to avoid the presence of a relatively small population of closed PS II reaction centers.

From the assignment of $\phi_{slow}$, the value of $\tau_{slow}$ is considered to be the average transfer time of an excited state from a closed reaction center to a neighboring open reaction center [42]. Therefore, the same value for $\tau_{slow}$ at $F_0$ and $F_{max}$ reflects the absence of communication between isolated PS II reaction centers, as in the absence of added cations or at pH values in the range 5.1–5.4. However, a shortening of $\tau_{slow}$ at $F_0$ is observed for structurally differentiated chloroplasts with an accompanying increase in $\tau_{slow}$ at $F_{max}$. These variations in $\tau_{slow}$ suggest the presence of energy transfer and of communication between PS II reaction centers as determined by the extent of domain formation. Thus, the data of Table IV, in agreement with earlier predictions, suggest that the smaller the hydrated metal ionic radius, the less extensive the domain formation needed for stacking and the lower the $F_{max}$ value of $\tau_{slow}$.

*Proposed model of cation effects on fluorescence decay kinetics*

We present the model of Fig. 12, to illustrate the origin of the chlorophyll fluorescence variations of stacked membranes in terms of structural variations of the grana, arising from differences in electrostatic screening effects of metal ions within the same valence group. In this model the screening ability of a given metal ion of specified valence is determined by the hydrated metal ionic radius and defines the extent of intermembrane separation as well as the associated lateral movement of chlorophyll-protein complexes. In general, the smaller the hydrated ionic radius, the more effective the electrostatic screening exhibited by the ion. Specifically, the smaller the hydrated ionic radius for metals of a given valency and at a given concentration, (1) the smaller the intermembrane distance across the partition gap of grana stacks, (2) the shorter the lateral distance between PS I and PS II complexes along the thylakoid membrane, and (3) the less extensive the antenna size or effective absorption cross-section of PS II complexes in the grana stacks. Thus, the more effective the electrostatic screening of a metal ion (as a consequence of its small hydrated ionic radius), the less differentiation between $\alpha$- and $\beta$-units. Note the similarity of this phenomenon to the mechanism of electrostatic neutralization whereby coulombic repulsion between adjacent membrane surfaces is decreased without the need for charge migration or the accompanying differentiation of PS II units [24,25]. More extensive lateral heterogeneity in the distribution of chlorophyll-protein complexes is predicted as hydrated metal-ion size increases. Although the model of Fig. 12 depicts only the extreme possibilities for the structure and organization of cation-induced stacked membranes, the entire range of intermediate stages is also possible.

The model depicted in Fig. 12 may also be used to illustrate that distinct cation effects on decay kinetics are generally observed at different concentration ranges, as previously noted [26,37]. We suggest that fluorescence variations which arise at low ion concentration (not more than 25 mM for monovalent ions and not more than 0.5 mM for divalent ions) are a consequence of membrane appression to intermediate separation distances not so great as to induce lateral segregation of PS I and PS II complexes. Furthermore, although small regions of stacked membranes develop, the electrostatic screening at low ion concentrations is not sufficient to allow aggregation of complexes along the membrane plane or to enable a close enough membrane approach to elicit complex aggregation. Thus, at low ion concentrations no changes in antenna size or extent of PS II to PS I energy

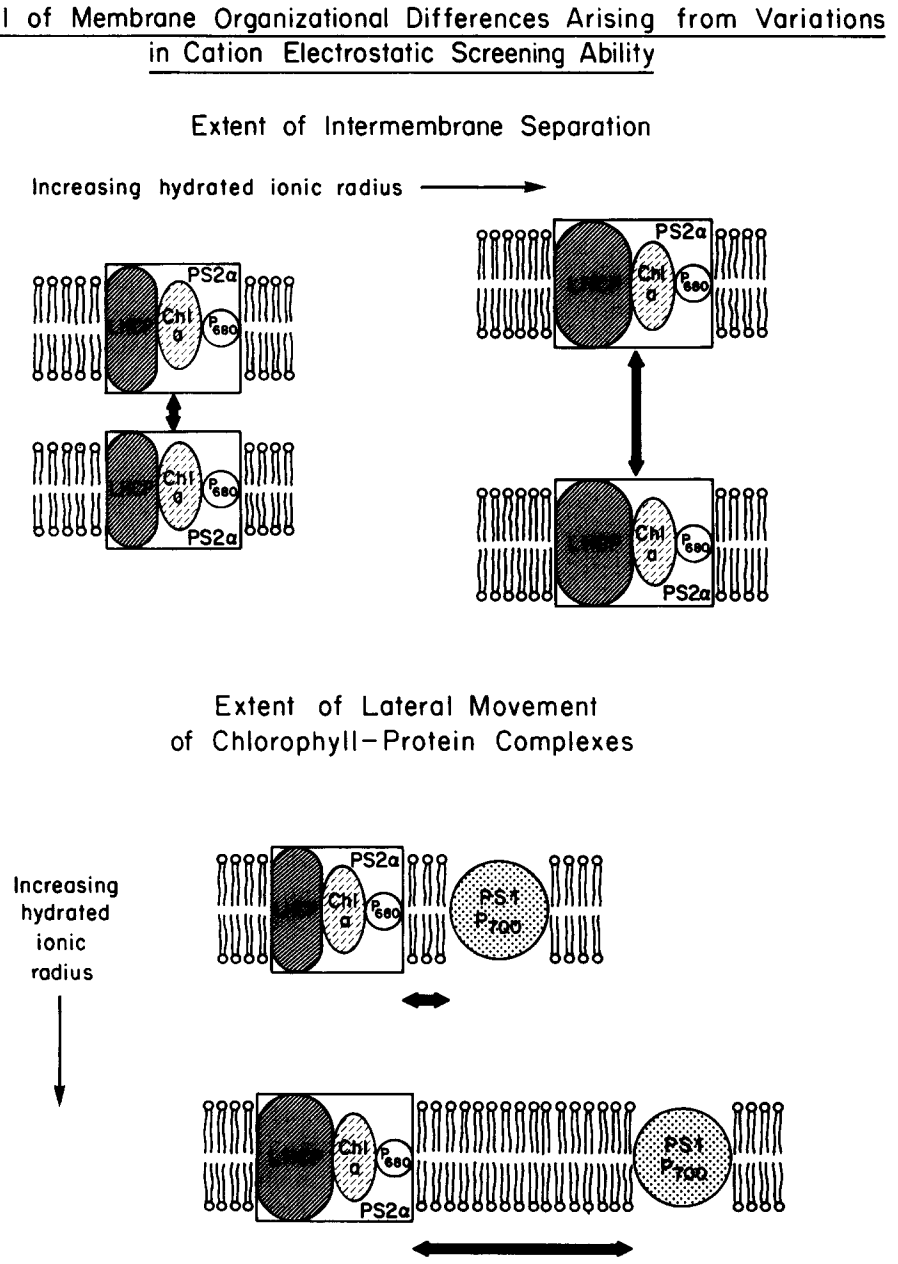


Fig. 12. Proposed model of the cation effects on intermembrane separation in grana stacks and on lateral segregation of Photosystems I and II. The symbols are defined as in Fig. 11.

transfer are expected from the membrane appression along the thylakoid surface. However, our present hypothesis supports a previous proposal by Staehelin and Arntzen [38], whereby at low salt concentrations the formation of 'pseudograna' occurs prior to the development of extensively stacked grana regions, providing some regions of membrane contact and the accompanying enhancement of PS II communication.

At higher ion concentrations (greater than 50 mM for monovalent ions and greater than 2 mM for divalent ions) a structural differentiation into

grana and stroma regions produces a spatial separation of photosystems as well as an increase in the PS II antenaa size in the grana partitions arising from the concentration of LHCP in stacked membranes. The transition from a state of isolated PS II units to one of interconnected complexes across partition gaps has also occurred at these higher concentrations. The redistribution of membrane components relieves energetically unfavorable repulsive forces arising from membrane stacking in accordance with Le Chatelier's principle [39]. For a given distance between membrane surfaces, the extent of reorganization is determined by the hydration force arising from the interaction of water shells structured around cations and around hydrophilic surface groups. The smaller the hydrated ionic radius, the less extensive the redistribution of membrane components needed and the closer the possible membrane approach. In other words, the weaker the hydration repulsion under conditions of cation screening, the more effective the Van der Waals attraction between opposing membranes, and the closer the approach of membrane surfaces without an extensive domain formation. The most extreme case occurs at low pH (approx. 5.1–5.4), where the component of the hydration repulsion which is due to the metal cations disappears, resulting in a net decrease of the distance between the thylakoid membranes or even a molecular contact at some points of the surface without any pigment-protein complex displacement [40,41].

## Conclusion

We have observed differential effects of cation-induced and pH-induced membrane stacking on the chlorophyll fluorescence decay kinetics of broken spinach chloroplasts and have related these differences to distinct stacking mechanisms of electrostatic screening and charge neutralization, respectively. Furthermore, we have distinguished variations in the cation effects of metals within the same valency group and have proposed that such variations are a consequence of differences in the screening ability of metal ions as influenced by the hydrated metal ionic radius. We have also proposed that differences in electrostatic screening exhibited by metals within the same valency group control the extent of intermembrane separation and the extent of the associated lateral movement of chlorophyll-protein complexes. We have proposed a model to associate the characteristics of the chlorophyll fluorescence decay kinetics with the structural organization of the photosynthetic apparatus and the degree of excitation transfer both between photosystems and among PS II units.

## Acknowledgments

This research was supported by the Director, Office of Energy Research, Office of Basic Energy Sciences, Division of Biological Energy Conversion and Conservation of the Department of Energy, under contract DE-AC03-76SF00098, and by a grant from the National Science Foundation (PCM82-10524). One of us (K.K.K.) wishes to acknowledge support through a National Institutes of Health National Research Service Award (1F32 GM08617) and a McKnight Foundation grant.

## References

1 Barber, J. (1976) in The Intact Chloroplast (Barber, J., ed.), pp. 89–134, Elsevier/North-Holland, Amsterdam
2 Barber, J. (1980) Biochim. Biophys. Acta 594, 253–308
3 Mercer, F.V., Hodge, A.J., Hope, A.B. and McLean, J.D. (1955) Aust. J. Biol. Sci. 8, 1–18
4 Nakatani, H.Y., Barber, J. and Forrester, J.A. (1978) Biochim. Biophys. Acta 504, 215–225
5 Nakatani, H.Y. and Barber, J. (1980) Biochim. Biophys. Acta 591, 82–91
6 Murata, N. (1969) Biochim. Biophys. Acta 189, 171–181
7 Murata, N., Tashiro, H. and Takamya, A. (1970) Biochim. Biophys. Acta 197, 250–256
8 Murata, N. (1971) Biochim. Biophys. Acta 245, 365–372
9 Homann, P. (1969) Plant Physiol. 44, 932–936
10 Murakami, S. and Packer, L. (1971) Arch. Biochem. Biophys. 146, 337–347
11 Barber, J. (1979) in Chlorophyll Organization and Energy Transfer in Photosynthesis, Ciba Found. Symp. 61, pp. 283–298, Elsevier/North-Holland, Amsterdam
12 Barber, J. (1980) FEBS Lett. 118, 1–10
13 Jennings, R.C., Garlaschi, F.M., Gerola, P.D., Etzion-Katz, R. and Forti, G. (1981) Biochim. Biophys. Acta 638, 100–107
14 Gross, E.L. and Prasher, S.H. (1974) Arch. Biochem. Biophys. 164, 460–468
15 Arntzen, C.J. and Briantais, J.M. (1975) in Bioenergetics of Photosynthesis (Govindjee, ed.), pp. 51–113, Academic Press, New York
16 Boardman, N.K., Anderson, J.M. and Goodchild, D.J. (1978) in Current Topics in Bioenergetics (Sanadi, D.R. and

Vernon, L.P., eds.), Vol. 8, pp. 35–109, Academic Press, New York
17 Anderson, J.M. (1982) Photobiochem. Photobiophys. 3, 225–241
18 Arntzen, C.J. (1978) in Current Topics in Bioenergetics (Sanadi, D.R. and Vernon, L.P., eds.), Vol. 8, pp. 111–160, Academic Press, New York
19 Andersson, B. and Anderson, J.M. (1980) Biochim. Biophys. Acta 593, 427–440
20 Anderson, J.M. (1981) FEBS Lett. 124, 1–10
21 Melis, A. and Thielen, A.P.G. (1980) Biochim. Biophys. Acta 589, 275–286
22 Barber, J. and Chow, W.S. (1979) FEBS Lett. 105, 5–10
23 Chow, W.S., Thorne, S.W., Duniec, J.T., Sculley, M.J. and Boardman, N.K. (1980) Arch. Biochem. Biophys. 201, 347–355
24 Scoufflaire, C., Lannoye, R. and Barber, J. (1982) Photobiochem. Photobiophys. 4, 249–256
25 Barber, J., Chow, W.S., Scoufflaire, C. and Lannoye, R. (1980) Biochim. Biophys. Acta 591, 92–103
26 Nairn, J.A., Haehnel, W., Reisberg, P. and Sauer, K. (1982) Biochim. Biophys. Acta 682, 420–429
27 Haehnel, W., Nairn, J.A., Reisberg, P. and Sauer, K. (1982) Biochim. Biophys. Acta 680, 161–173
28 Leskovar, B., Lo, C.C., Hartig, P.R. and Sauer, K. (1976) Rev. Sci. Instrum. 47, 1113–1121
29 Hartig, P.R., Sauer, K., Lo, C.C. and Leskovar, B. (1976) Rev. Sci. Instrum. 47, 1122–1129
30 Turko, B.T., Nairn, J.A. and Sauer, K. (1983) Rev. Sci. Instrum. 54, 118–120
31 Bevington, P.R. (1969) in Data Reduction and Error Analysis for the Physical Sciences, p. 89, McGraw-Hill, New York
32 Karukstis, K.K. and Sauer, K. (1983) Biochim. Biophys. Acta 722, 364–371
33 Breton, J. and Geacintov, N. (1980) Biochim. Biophys. Acta 594, 1–32
34 Karukstis, K.K. and Sauer, K. (1983) J. Cell. Biochem. 23, 131–158
35 Melis, A. and Ow, R.A. (1982) Biochim. Biophys. Acta 682, 1–10
36 Melis, A. and Duysens, L.N.M. (1979) Photochem. Photobiol. 29, 373–382
37 Henkin, B.M. and Sauer, K. (1977) Photochem. Photobiol. 26, 277–286
38 Staehelin, L.A. and Arntzen, C.J. (1979) CIBA Found. Symp. 61, 147–169
39 Israelachvili, J.N. (1978) in Light Transducing Membranes (Deamer, D.N., ed.), pp. 91–107, Academic Press, New York
40 Thorne, S.W. and Duniec, J.T. (1983) Quart. Rev. Biophys. 16, 197–278
41 Duniec, J.T., Israelachvili, J.N., Ninham, B.W., Pashley, R.M. and Thorne, S.W. (1981) FEBS Lett. 129, 193–196
42 Haehnel, W., Holzwarth, A.R. and Wendler, J. (1983) Photochem. Photobiol. 37, 435–443